International Journal of Heat and Mass Transfer 51 (2008) 6032–6038

Contents lists available at ScienceDirect

International Journal of Heat and Mass Transfer

journal homepage: www.elsevier.com/locate/ijhmt

Determination of the heat transfer coefficient at metal–die interface of high pressure die casting process of AM50 alloy

Guo Zhi-peng [a], Xiong Shou-mei [a,*], Liu Bai-cheng [a], Mei Li [b], John Allison [b]

[a] Key Laboratory for Advanced Manufacturing by Materials Processing Technology, Department of Mechanical Engineering, Tsinghua University, Beijing 100084, China
[b] Research and Advanced Engineering Department, Scientific Research Laboratory, Ford Motor Company, Dearborn, MI 48121, USA

ARTICLE INFO

Article history:
Received 30 September 2007
Received in revised form 11 April 2008
Available online 7 June 2008

Keywords:
High pressure die casting
Interfacial heat transfer coefficient
AM50 alloy
Process parameters

ABSTRACT

This paper focuses on the determination of the interfacial heat transfer coefficient (IHTC) at the metal–die interface in the high pressure die casting (HPDC) process. Experiment was conducted and a "step shape" casting was used to cast a magnesium alloy AM50 against a H13 steel die. Based on the temperature measurements inside the die, IHTC was determined by applying an inverse approach. The influences of the step thickness and process parameters on the IHTC were investigated. Results show that the shape of IHTC profiles is different at different steps and the duration for IHTC to maintain a higher value grows as the step thickness increases. The influence of process parameters is mainly on the IHTC peak value. For thinner steps, a higher fast shot velocity leads to a higher IHTC peak value. But for thicker steps such as Step 5, the casting pressure shows a more prominent influence on the IHTC peak value. Also, at these thicker steps a lower initial die surface temperature always leads to a higher IHTC peak value.

1. Introduction

Magnesium alloy castings have been extensively used in the automotive industry in the past few years. The primary reason for this is the lightness of magnesium – one-third lighter than aluminum, three-quarters lighter than zinc and four-fifths lighter than steel [1]. Most magnesium alloy components presently are produced by the high pressure die casting process (HPDC), which is one of the most growing and efficient methods for the production of complex shape castings in today's manufacturing industry. But defects such as shrinkage and gas pores are often observed in the cast parts. These defects deteriorate the mechanical properties of the casting components, which greatly limits the application of magnesium alloys.

In the HPDC process, the molten metal is forced to fill the die cavity by a piston in a very short period and solidify under a high pressure before the complete solidification of the thin gate. Such pressure is several orders of magnitude greater than the melt pressure in conventional casting processes. The die is usually manufactured from hardened steels and the cast metals are predominantly low melting point alloys such as aluminum and magnesium alloys.

Modeling of solidification can be of great benefit in improving the efficiency of the die casting process by showing how solidification defects can be avoided. Good models require accurate boundary conditions as well as the thermal properties of the materials involved and the initial conditions of the casting and the die. Among all the boundary conditions, of central importance is the heat transfer coefficient at the metal–die interface during the solidification process because of its marked influence on the microstructure of the casting.

Determination of the interfacial heat transfer coefficient (IHTC) is classically performed with measurements of the temperatures in the die and in the casting. The experimental results are then either compared to numerical simulation results with fitted interfacial parameters or obtained with an inverse model of the transient heat transfer. The interface is usually regarded as a layer of thermal resistance [2,3] and the heat transfer coefficient can be determined by the division between the interfacial heat flow density and the temperature difference of the casting and die surface temperatures.

For decades, researchers have strived to obtain heat transfer coefficients for different metal-mold interfaces and processes experimentally, analytically or with inverse modeling approaches [4–21]. However, most of the work so far has been focused on sand or permanent mold casting processes, and there is very limited knowledge about interfacial heat transfer during the solidification of the HPDC process.

Dour et al. [22,23] studied the requirements for accurate determination of the heat transfer coefficient during rapid forming processes. They recommended that some requirements including the fast sensor response, proper location of the sensor, and proper way of applying the inverse method must be met in order to accurately determine the IHTC. In HPDC process, at a time between a few tens to a few hundreds of milliseconds after filling, high pressure is effective, which forces the melt into close conformity with

* Corresponding author. Tel.: +86 010 62773793.
E-mail address: smxiong@tsinghua.edu.cn (X. Shou-mei).

0017-9310/$ - see front matter © 2008 Elsevier Ltd. All rights reserved.
doi:10.1016/j.ijheatmasstransfer.2008.04.029

the die surface. In such a short period the thermocouple used to measure the temperature must respond fast enough to follow the various stages carried out in a HPDC cycle. In order to apply the inverse method successfully, it is also necessary to optimize the location of the thermocouples and particularly the one closest to the interface.

Nelson [24] used four thermocouples located near the casting/die interface to determine the IHTC for the die casting of the magnesium alloy AZ91B. The average IHTC value was estimated to be 19,624 W m^{-2} K^{-1} during the solidification of the casting. Hong et al. [25] determined the IHTC during the HPDC process by casting an A380-based alloy flat plate casting. By comparing the measured and simulated temperatures, they found that the best match was achieved when the average heat transfer coefficient 79,400 W m^{-2} K^{-1} was employed. Papai and Mobley [26] conducted die casting experiments using an A380 aluminum alloy bowl-shaped casting and an H13 steel die. An iterative procedure first used by Beck [27] was used to treat the measured thermal field in the die.

Most recently, Dour et al. [23] reported their work on developing a non-intrusive heat transfer gauge and its application in the HPDC to evaluate IHTC of a thin wall aluminum casting. The results showed that a higher fast shot velocity and a lower initial die temperature led to a higher IHTC peak value. Casting pressure and other process parameters, on the other hand, had little influence on the IHTC. Hamasaiid et al. [28] also found that the fast shot velocity and the initial temperature of the die have a great influence on the IHTC peak values.

Most of the previous work concentrated on the determination of the IHTC under various operation conditions in the HPDC process. There have been very few reports on the influence of the casting thickness on the IHTC. Also, little attention was paid on the influence of the process parameters on the IHTC at different locations on a casting especially the one with different thicknesses. As such, a comprehensive understanding of the influence of the casting thickness on IHTC is an important and urgent issue.

By applying a "step shape" casting with different thicknesses, the approach of this work was (1) to determine the IHTC of a commercial magnesium alloy, AM50, under the HPDC solidification process; (2) to investigate the influence of the casting thickness on the heat transfer coefficient; and (3) to further study the influences of various process parameters (such as the casting pressure, the fast shot velocity, the pressure intensification time, the die temperature, and the melt temperature) on the IHTC at these different steps.

2. Experiments

2.1. "Step shape" casting

A specially designed casting namely "step shape" casting was used in the current study. As shown in Fig. 1, the "step shape" casting has five steps with different thicknesses from Step 1, of 2 mm, to Step 5, of 14 mm, with intervals of 3 mm.

2.2. Die configuration and sensor installation

The installation of the thermocouples is a very difficult task. Hong et al. [25] reported two difficulties in placing thermocouples in holes drilled from the rear of the die toward the casting-die interface. The first is that the exact distance between the temperature measurement point and the casting-die interface is very hard to measure. The other difficulty is that it is hard to ensure that the thermocouple tip is securely attached to the die. As mentioned in Ref. [22] and discussed in our previous work [29], for rapid forming processes such as the HPDC process, a small uncertainty in the location of the thermocouple can lead to serious mistakes in the determination results.

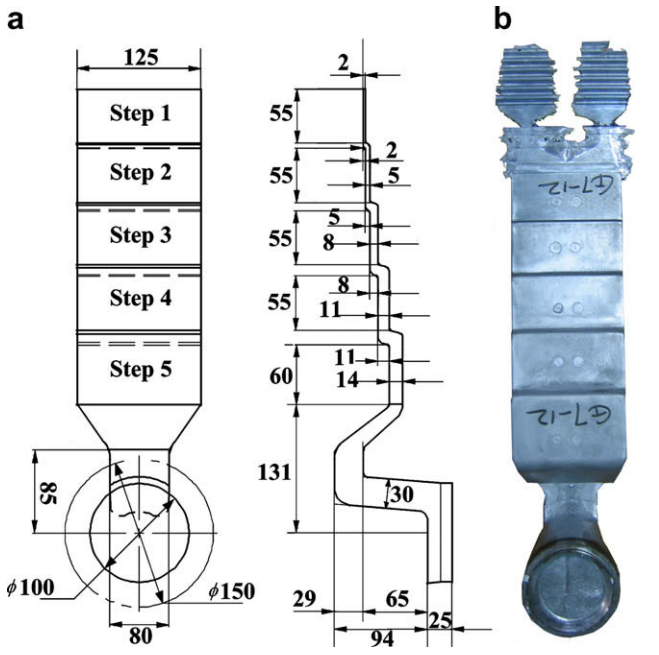

Fig. 1. "Step shape" casting: (a) size and geometry; (b) actual casting.

In order to overcome the uncertainty in the installation of the thermocouples, a special temperature sensor unit was developed. As shown in Fig. 2, six 0.8 mm-wide and 1 mm-deep grooves were machined into the sensor unit for the placement of the thermocouples. The grooves were machined to terminate at the appropriate distance (1 mm, 3 mm and 6 mm) from the front wall of the sensor unit. Six thermocouples were laid into the grooves and each thermocouple tip was welded to the end wall of the groove.

The thermocouples were sheathed K-type thermocouples with a thermocouple wire diameter of 0.1 mm. A boiling water test was performed and the response time (defined in Ref. [30]) of thermocouple was estimated to be about 7–10 ms according to the results obtained from a set of ten thermocouples. Under such conditions, according to Refs. [22,29], the difference between the measured temperature and the actual temperature can be negligible.

Fig. 3 shows the configuration of the dies that were used during the experiment. Five temperature sensor units, designated S_T1–S_T5, were installed into the fixed die at different locations. Each of these temperature sensor units was used to measure the die temperatures at each step. The sensor unit was manufactured using the same material as the die to ensure that the heat transfer process would not be distorted. Each sensor unit was adjusted into the die until the front wall of the sensor unit approached the cavity surface.

2.3. Casting conditions

A TOYO 650t cold chamber die casting machine was used in the present work. Nearly 290 shots were performed under all the operation conditions. The process parameters that were varied during the experiment included the casting pressure (P), the fast shot velocity (V_H), the die temperature (T_m), the pressure intensification time (t_{In}), and the melt temperature of the alloy (T_P). Seven shots were repeated under each operation condition. The casting material was AM50 alloy with a chemical composition as (wt.%): Al (5.05%), Zn (<0.02%), Mn (0.23%), Si (0.041%) and Fe (0.003%). The

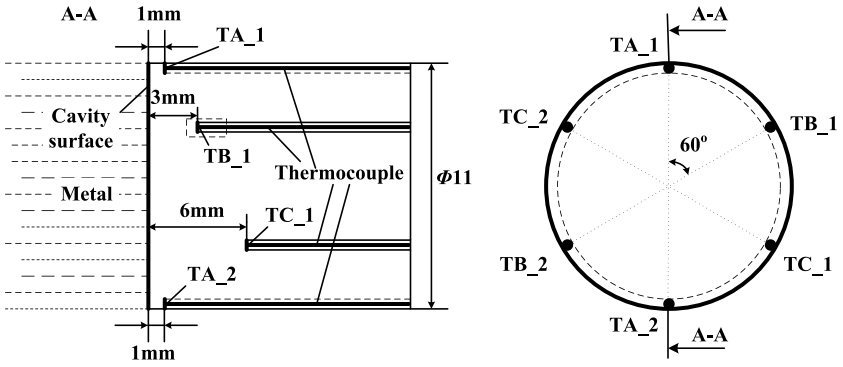

Fig. 2. Configuration of the temperature sensor unit.

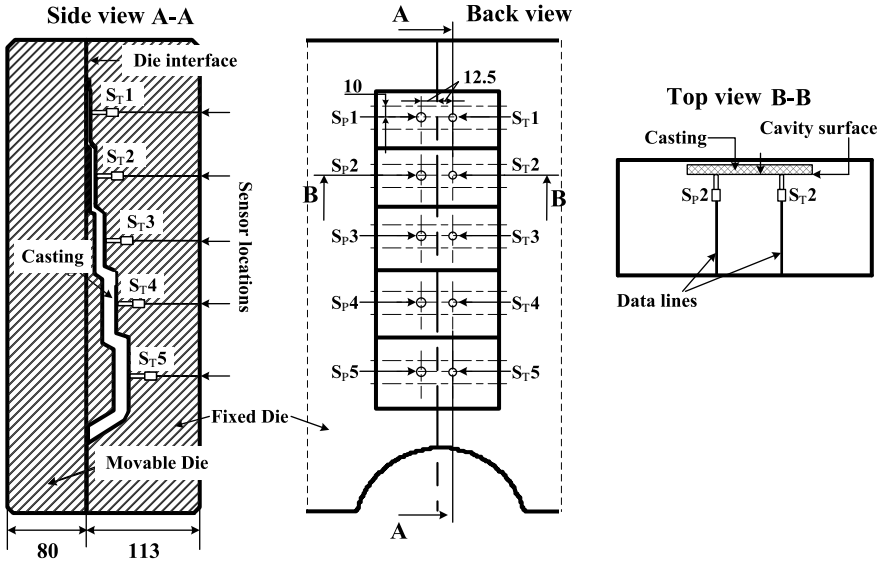

Fig. 3. Configuration of the dies and adjustment of the temperature sensor units.

Table 1
Thermal property of the related materials

Thermal properties	AM50	H13
Thermal conductance λ (W m^{-1} K^{-1})	62	31.2–0.013T*
Specific heat C_P (J kg^{-1} K^{-1})	1050	478–0.219T
Density ρ (kg m^{-3})	1780	7730–0.24T
Liquidus temperature T_L (°C)	628	1471
Solidus temperature T_S (°C)	546	1404
Latent heat L (J kg^{-1})	373,000	209,350

* T stands for temperature (°C).

die material was H13 and lubrication was performed with Deltacast 333 manufactured by Acheson. The related thermal property data is shown in Table 1.

A data logger manufactured by Integrated Measurement Corporation (IMC) was used with a high data sampling rate of 200 Hz, in order to meet the requirements for the determination of the IHTC in the HPDC process. Further discussion of this can be found in Refs. [22,29].

3. Heat transfer evaluation

Based on the temperature measurements at 1 mm (average of TA_1 and TA_2) and 6 mm (average of TC_1 and TC_2) from the cavity surface, IHTC was determined using an inverse approach introduced by Beck [27,31,32]. The inversely determined temperatures at 3 mm from the cavity surface are compared to the measured temperatures at TB series to validate the inverse modeling.

The filling time in HPDC process is always two or three orders of magnitude shorter than the solidification time; therefore the filling process is regarded as "instant filling". Also, due to the fact that the casting step is much thinner than the die and the main interest of the present paper is on the heat transfer at the metal–die interface during the solidification process, during the estimation of the casting's thermal field the following assumptions were made: (1) the heat transfer at each step is one-dimensional; (2) the step center is adiabatic and (3) the initial temperature of the casting is the melt temperature.

A typical set of measured temperature curves inside the die of Step 3 are shown in Fig. 4a. Designated by TA3_1, TA3_2, TC3_1 and TC3_2, the temperatures were measured under a casting pressure of 67 MPa, a slow shot velocity of 0.2 ms^{-1}, a fast shot velocity of 2 ms^{-1}, and a pressure intensification time of 40 ms, which is referred to as the reference condition in the following text for convenience. The melt temperature T_P and the die temperature T_m were maintained at 680 °C and 150 °C prior to casting.

As shown in Fig. 4a, the temperature curves measured at the same distance in the sensor unit, such as TA3_1 and TA3_2 or TC3_1 and TC3_2, almost overlapped, indicating that the heat transfer process can be reasonably assumed to be one-dimensional. Based on the measured temperatures, the die surface

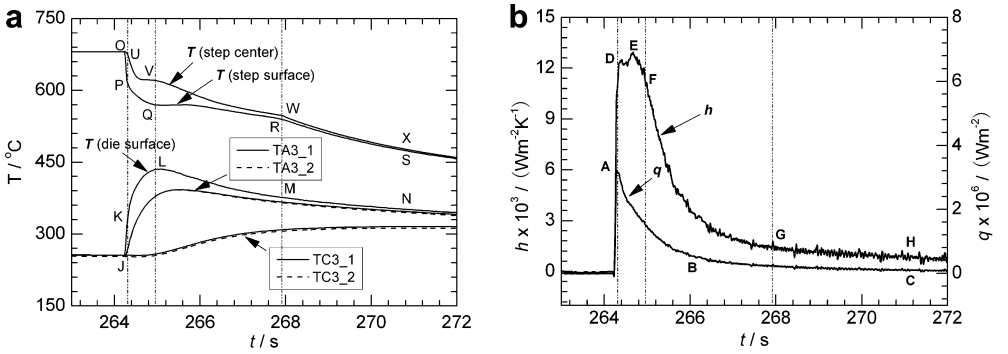

Fig. 4. (a) Measured temperatures and determined step center and surface temperatures (b) determined IHTC and heat flux at Step 3 under the reference condition.

temperature, step center and surface temperatures designated by T (die surface), T (step center) and T (step surface) as shown in Fig. 4a were determined by applying the inverse approach. The measure and simulated temperatures at 3 mm (TB) show a good agreement and a maximum difference of about 4 °C was found between these two temperature profiles indicating that the determined results were quite reliable.

Segment OP of T (step surface) represents the period immediately after metal pouring. The abrupt negative slope of this segment indicates a fast heat transfer at the metal–die interface. The rapid decrease of the step surface temperature occurred in the first 70 ms of metal solidification indicating a high cooling rate of Step 3. In tandem with such decrease, it is noted in Fig. 4a that there is a corresponding increase in the die surface temperature as designated by segment JK. After segment OP, the step surface temperature was followed by a continuous decrease designated by the segment PQ. Comparing OP, segment PQ indicates a much smaller cooling rate of Step 3, as is also evident in Fig. 4a from the smaller slope of curve T (die surface), designated by segment KL. The casting at Step 3 kept losing its heat until it was completely solidified, which is denoted by point W at the T (step center) curve.

Fig. 4b shows the determined IHTC (h) and heat flux (q) profiles associated with the results in Fig. 4a. Corresponding to the rapid decrease of the step surface temperature (segment OP) the IHTC increased abruptly immediately after the shot was performed until reaching a value of about 10,456 W m^{-2} K^{-1}. This abrupt increase was also associated with the rapid increase in the heat flux until its maximum value (Fig. 4b, point A, 3.22 MW m^{-2}) was reached. The IHTC kept growing until reaching 12,278 W m^{-2} K^{-1} (Fig. 4b, point D) when the IHTC started to fluctuate, rising and falling until it approached point F, after which the IHTC dropped rapidly until its value was less than 1000 W m^{-2} K^{-1}. The abrupt decrease of the IHTC designated by segment FGH was due to the fact that the close contact formerly achieved between the casting and the die was deteriorated, which is probably caused by the lack of the required pressure transferred from inside as the solidification process proceeded. Analysis of the heat flux curve enables us to find that after the maximum value has arrived, the heat flux experienced an exponential decay until its value was at a much lower level as designated by the segment ABC.

Fig. 5 shows the calculated IHTC at Step 1 to Step 5 under the reference condition. All the other IHTC profiles change in a similar manner as that at Step 3 as discussed before. The IHTC always underwent an initial abrupt increasing stage immediately after the shot was performed until reaching its maximum value, and then decreased until its value was at a much lower level. However, it takes longer time for IHTC to decrease to such a lower value as the step thickness increases, which can be clearly concluded by comparing the arriving time of point G as shown in Fig. 5. Also, as can be seen from Fig. 5, the casting thickness greatly affected

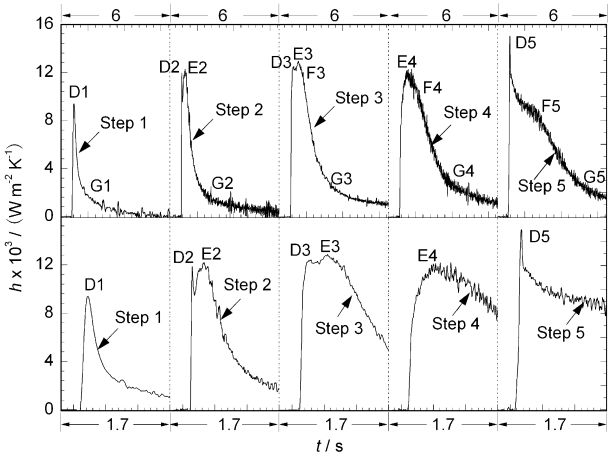

Fig. 5. Determined IHTC profiles at Steps 1–5 under the reference condition.

the shape of the IHTC profile. The thinner the step, the slimmer the IHTC profile.

Comparing the results of Step 3, the IHTC at Step 4 changes a little different: it took more than 0.4 s for the IHTC to climb to its maximum value of about 11,820 W m^{-2} K^{-1}. This time period is much longer than those of other steps which according to the current results are always less than 0.1 s. This delayed maximum value directly results in that there is no explicit initial increasing stage (in other words there is no explicit point D4) on the IHTC profile at Step 4. Such characteristic is also different from the results from Step 5 at which a clear initial increasing stage can be observed according to Fig. 5. However, it can also be seen that after the initial increasing stage the IHTC at Step 5 dropped in a much faster rate and followed by a continuous decrease until its value was at a much lower value. This abrupt and continuous decrease of IHTC is quite different from most of the other steps such as Step 2, Step 3 and Step 4 but more similar to the situation of Step 1.

The difference of the IHTC profiles discussed above may be understood by considering the flow pattern of the "step shape" casting. As shown in Figs. 1 and 3, the melt alloy flowed into the cavity of Step 5 from the gating system in a direction which is toward the surface of the fixed die where the temperature sensor units were installed. The melt alloy maintained its flow path along the surface of the fixed die until reaching the cavity of Step 4 where the direction of the flow changed because of the transition from Step 5 to Step 4. In other words, when the melt entered the cavity of Step 4 it flushed toward the surface of the movable die instead of the fixed die where the sensor unit was installed, which consequently leads to an indirect impact between the melt and the front wall of the sensor unit at Step 4. The heat transfer during the initial

increasing stage may be dependent on such filling behavior. As a result, the indirect flush toward the fixed die surface at Step 4 leads to an inconspicuous maximum value of the IHTC during the initial increasing stage. Also, because of the direct impact from the melt to the fixed die surface at Step 5 a prominent initial increasing stage of IHTC can be well formed. As is also mentioned in reference [33], the maximum value of the determined IHTC is greatly dependent on the status of the contact between the melt alloy and the die surface where the thermocouples are installed. A higher IHTC peak value was observed when the melt alloy directly hit the location below which the thermocouples were adjusted during their initial contact.

Given that the flow direction of the melt at Steps 1–3 is similar to that at Step 4. The initial increasing stage of IHTC at these steps must be also influenced by the filling pattern of the melt. However, such influence must be less intense as the step becomes thinner. This explains the fact that the change tendency of the IHTC at Step 5 is more similar to that at Step 1 rather than the other steps.

4. Influence of process parameters

Fig. 6 shows the determined IHTC profiles at Steps 1–5 under different casting pressures of 24 MPa, 44 MPa and 67 MPa, respectively. Other process parameters were kept the same as the reference condition. Each IHTC profile was the average of the sequential seven curves determined under each condition.

According to Fig. 6, casting pressure has little influence on the shape of the IHTC profile, and within a particular step the only difference of the IHTC is the peak value. Similar phenomenon can also be found on the IHTC profiles when other process parameters such as fast shot velocity, pressure intensification time, pouring temperature and die temperature were varied. As such, the following discussion (for investigating the influence of the process parameters on IHTC) is mainly emphasizing at the IHTC peak values rather than the whole IHTC profile.

Investigation of the influence of die temperature on IHTC brings a little challenge, since the die temperature changed as the solidification of the casting proceeded. According to our study, we found that the initial die surface temperature (the die surface temperature prior to the shot) could in some way characterize the degree that the IHTC peak value changed.

Fig. 7a shows the IHTC peak values of each shot at the five steps under all the operation conditions and Fig. 7b shows the corresponding initial die surface temperature (T_{DI}) at each step. For each set of tests only one process parameter was changed and labeled in the figure. The other parameters were kept the same as the reference condition.

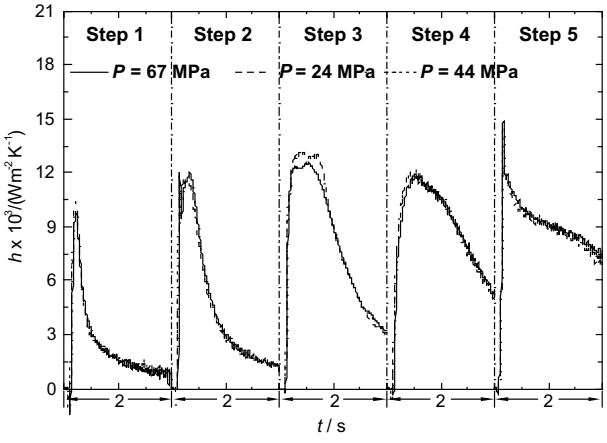

Fig. 6. Determined IHTC profiles under different casting pressures (24 MPa, 44 MPa and 67 MPa).

As shown in Fig. 7a, the influence of process parameters on the IHTC peak values seems very arbitrary and such influence is further complicated with the change of the step thickness. As shown in Fig. 7b, all the T_{DI} values changed in a similar manner and the only difference of the T_{DI} at these different steps appears to be the temperature value. The T_{DI} values of the thicker steps like Steps 3, 4 and Step 5 were always higher than those of the thinner steps like Steps 1 and 2. The similar trend of these temperatures indicates that a thermal equilibrium was achieved inside the die.

For the thinner steps like Step 1 and Step 2, the fast shot velocity seriously affected the IHTC peak values. As shown in the top two layers of Fig. 7a, the upright hollow triangles, which characterize the IHTC peak values obtained under a fast shot velocity of 4 ms^{-1}, are always located above the upside-down hollow triangles, which characterize the IHTC peak values obtained under a fast shot velocity of 0.7 ms^{-1}. Through six sets of tests as the sequence advanced, the IHTC peak values under a higher fast shot velocity were always higher than those obtained when the fast shot velocity was lower. In comparison of the IHTC peak values under the fast shot velocity of 0.7 ms^{-1} and 4 ms^{-1}, a clear difference of about 1000–2000 W m^{-2} K^{-1} can be observed in the case of Step 1, and a range of 2000–3000 W m^{-2} K^{-1} can be observed in the case of Step 2. Other process parameters such as the casting pressure, the pressure intensification time and the melt temperature have little influence on the IHTC peak values at Step 1 and Step 2.

From the third layer of Fig. 7a, it can be seen that process parameters such as casting pressure, fast shot velocity and pressure intensification time had very little influence on the IHTC peak values at Step 3. All the IHTC peak values are mixed though a prominent distinction (about 1500 W m^{-2} K^{-1}) can be observed when the fast shot velocity was increased from 0.7 ms^{-1} to 4 ms^{-1} during the initial stage of the experiment. The IHTC peak values decreased as successive cycles were performed. As shown in Fig. 7a, the IHTC peak values at Step 3 were about 14,000 W m^{-2} K^{-1} at the beginning of the casting process under the reference condition. As the cycles were sequentially performed, the peak values had decreased as much as 1600 W m^{-2} K^{-1} at the end of the experiment, when the melt temperature was 680 °C. Comparing this change trend with the sequentially increasing T_{DI} values shown in Fig. 7b at Step 3, it can be found that the IHTC peak values decrease as the initial die surface temperatures increase. Such relationship between the IHTC peak value and the initial die surface temperature also exists at the results at Step 5. As shown in the bottom layer of Fig. 7a, the average of the IHTC peak values of the first seven shots of the reference condition is about 18,200 W m^{-2} K^{-1}, which is much higher than the value about 14,000 W m^{-2} K^{-1} of the last seven shots of the reference condition when the melt temperature is 680 °C. This phenomenon indicates that the initial die surface temperature has an impact on the IHTC peak values and the thicker the step is the more prominent such influence becomes.

Despite of the influence of the initial die surface temperature, the IHTC peak values at Step 5 were also influenced by the casting pressure. The IHTC peak values under a casting pressure of 24 MPa, characterized by the hollow triangles pointing left, were always lower than those obtained when the casting pressure was 67 MPa, characterized by the upright solid triangles. But such difference became more and more indistinguishable as successive castings were performed. For example, the average difference between the IHTC peak values obtained under the casting pressure of 24 MPa and 67 MPa was about 5000 W m^{-2} K^{-1} during the sequences performed at the start of the experiment but less than 1000 W m^{-2} K^{-1} at the end of the shot sequences, when the melt temperature was 680 °C.

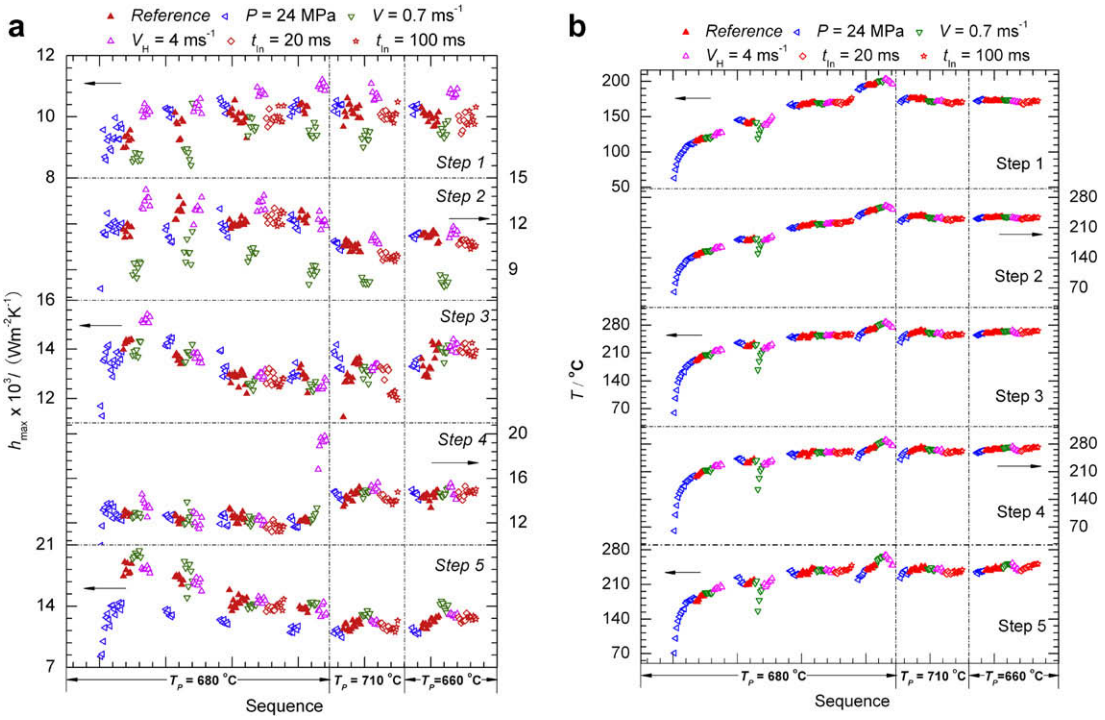

Fig. 7. (a) IHTC peak values (b) initial die surface temperature of each shot at Steps 1–5.

The IHTC peak values at Step 4 changed more dramatically than the other steps. All the IHTC peak values remained at about 12,000 W m^{-2} K^{-1} when the melt temperature was 680 °C except those when the fast shot velocity was 4 ms^{-1}, under which the IHTC peak values climbed to almost 20,000 W m^{-2} K^{-1}. After such abrupt change, the IHTC peak values remained at about 15,000 W m^{-2} K^{-1} whether the melt temperature was 710 °C or 660 °C. But such value was still higher than those obtained at the former sequences when the melt temperature was 680 °C. Fig. 8 shows the IHTC profiles at Step 4 corresponding to this abrupt change. It is notable that an abrupt initial increasing stage appears at Curve 1 which was obtained when V_H is 4 ms^{-1} and T_P is 680 °C. This situation is quite different from that as shown in Fig. 5. Such abrupt increasing stage of IHTC directly leads to a huge maximum value which is about 19,200 W m^{-2} K^{-1} according to Fig. 8. After this peak value, the IHTC kept falling and gradually converged to the other two curves namely Curve 2 and Curve 3. This abrupt increase at the initial stage is more similar to the result at Step 5. The appearance of the abrupt increase at the initial stage of the IHTC must be caused by the improvement of the contact between the melt and the die at Step 4. But the exact reason for this is not quite clear yet.

The IHTC peak values at Steps 1–5 did not change prominently even the pressure intensification time was varied from 20 ms to 100 ms. Also, according to Fig. 7a, the variation of the melt temperature had not brought a prominent affect on the IHTC peak values.

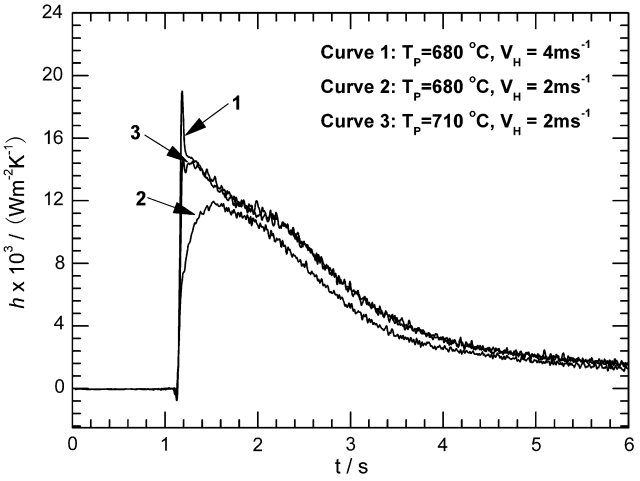

Fig. 8. IHTC profiles at Step 4 corresponding to the abrupt change of the IHTC peak values shown in Fig. 7a.

5. Conclusion

The IHTC between a commercial magnesium alloy AM50 casting and a H13 steel die in the HPDC process was successfully determined based on the temperature measurements during the die casting experiment. A "step shape" casting was used and a temperature sensor unit was designed in order to make accurate temperature measurement in the HPDC process.

The step thickness has a great influence on the shape of the IHTC profile. The thinner the step, the slimmer the IHTC profile. The duration for the IHTC to maintain a higher value grows as the step thickness increases.

Process parameters only influence the peak value of the IHTC, but such influence is further complicated with the change of the step thickness. The IHTC peak values of the thinner steps such as Step 1 and Step 2 are more dependent on the fast shot velocity rather than the other process parameters. The higher the fast shot velocity, the higher the IHTC peak values at these two steps. Casting pressure has a more pronounced influence on the IHTC peak values at Step 5. Extra intensification pressure greatly enhances the maximum values of the IHTC at Step 5. However, such influence becomes more indistinguishable as the initial die surface temperature rises. The results also show that the IHTC peak values are

higher when the initial die surface temperature is lower. But such phenomenon was only observed prominently under the cases of Step 3 and Step 5.

The flow pattern of the melt may in some way affect the IHTC especially the initial increasing stage as can be observed by the dramatic change of the IHTC at Step 4. The characteristic of the IHTC at Step 5 also indicates the existence of such influence. The basic mechanism of this is not clear and needs further investigation.

It should be noted that during the estimation of the casting thermal field, the present paper made an assumption that the initial temperature of the casting equals to the melt temperature. However, the metal temperature would drop due to the heat loss during the slow shot period (when the metal is in the sleeve). Consequently, the determination procedure in the current study could lead to an underestimate of the IHTC.

Acknowledgements

This research was financially supported by National Science Foundation of China (50675114) and National Basic Research Program of China (2006CB605208-2). The experimental work was conducted at Tsinghua-TOYO R&D Center of Magnesium and Aluminum Alloys Processing Technology with the help of engineers from TOYO Machinery & Metal Co., Ltd.

References

[1] H. Hu, A. Yu, Numerical simulation of squeeze cast magnesium alloy AZ91D, Modell. Simul. Mater. Sci. Eng. 10 (1) (2002) 1–11.
[2] K. Ho, R.D. Pehlke, Metal-mold interfacial heat transfer, Metall. Mater. Trans. B: Process Metall. Mater. Process. Sci. 16B (3) (1985) 585–594.
[3] K. Ho, R.D. Pehlke, in: AFS (Ed.), Transactions of the American Foundrymen's Society, Proceedings of the Eighty-Seventh Annual Meeting, AFS, Des Plaines, Rosemont, IL, 1983, pp. 689–698.
[4] Y. Nishida, W. Droste, S. Engler, Air-gap formation process at the casting-mold interface and the heat transfer mechanism through the gap, Metall. Mater. Trans. B: Process Metall. Mater. Process. Sci. 17B (4) (1986) 833–844.
[5] D.G.R. Sharma, M. Krishnan, in: AFS (Ed.), Proceedings of the 95th Annual Meeting of the Transactions of the American Foundrymen's Society, American Foundrymen's Society, Des Plaines, Chicago, IL, 1991, pp. 429–433.
[6] M. Krishnan, D.G.R. Sharma, Determination of the interfacial heat transfer coefficient *h* in unidirectional heat flow by Beck's non linear estimation procedure, Int. Commun. Heat Mass Transfer 23 (2) (1996) 203–214.
[7] R.W. Lewis, R.S. Ransing, Correlation to describe interfacial heat transfer during solidification simulation and its use in the optimal feeding design of castings, Metall. Mater. Trans. B: Process Metall. Mater. Process. Sci. 29 (2) (1998) 437–448.
[8] F. Lau, W.B. Lee, S.M. Xiong, B.C. Liu, Study of the interfacial heat transfer between an iron casting and a metallic mould, J. Mater. Process. Technol. 79 (1–3) (1998) 25–29.
[9] W.D. Griffiths, Heat-transfer coefficient during the unidirectional solidification of an Al–Si alloy casting, Metall. Mater. Trans. B: Process Metall. Mater. Process. Sci. 30 (3) (1999) 473–482.
[10] W.D. Griffiths, Model of the interfacial heat-transfer coefficient during unidirectional solidification of an aluminum alloy, Metall. Mater. Trans. B: Process Metall. Mater. Process. Sci. 31 (2) (2000) 285–295.
[11] S. Broucaret, A. Michrafy, G. Dour, Heat transfer and thermo-mechanical stresses in a gravity casting die Influence of process parameters, J. Mater. Process. Technol. 110 (2) (2001) 211–217.
[12] C.A. Santos, J.M.V. Quaresma, A. Garcia, Determination of transient interfacial heat transfer coefficients in chill mold castings, J. Alloys Compd. 319 (1–2) (2001) 174–186.
[13] R.I.L. Guthrie, M. Isac, J.S. Kim, R.P. Tavares, Measurements, simulations, and analyses of instantaneous heat fluxes from solidifying steels to the surfaces of twin roll casters and of aluminum to plasma-coated metal substrates, Metall. Mater. Trans. B: Process Metall. Mater. Process. Sci. 31 (5) (2000) 1031–1047.
[14] G.X. Wang, E.F. Matthys, Experimental determination of the interfacial heat transfer during cooling and solidification of molten metal droplets impacting on a metallic substrate: Effect of roughness and superheat, Int. J. Heat Mass Transfer 45 (25) (2002) 4967–4981.
[15] C.P. Hallam, W.D. Griffiths, A model of the interfacial heat-transfer coefficient for the aluminum gravity die-casting process, Metall. Mater. Trans. B: Process Metall. Mater. Process. Sci. 35 (4) (2004) 721–733.
[16] S. Jayanti, M. Valette, Prediction of dryout and post-dryout heat transfer at high pressures using a one-dimensional three-fluid model, Int. J. Heat Mass Transfer 47 (22) (2004) 4895–4910.
[17] J.A. Hines, Determination of interfacial heat-transfer boundary conditions in an aluminum low-pressure permanent mold test casting, Metall. Mater. Trans. B: Process Metall. Mater. Process. Sci. 35 (2) (2004) 299–311.
[18] A.S. Sabau, in: TMS (Ed.), TMS Light Metals, Minerals, Metals and Materials Society, San Antonio, TX, 2006, pp. 827–832.
[19] G. Kumar, S. Hegde, K.N. Prabhu, Heat transfer and solidification behaviour of modified A357 alloy, J. Mater. Process. Technol. 182 (1–3) (2007) 152–156.
[20] T.S.P. Kumar, K.N. Prabhu, Heat flux transients at the casting/chill interface during solidification of aluminum base alloys, Metall. Mater. Trans. B: Process Metall. Mater. Process. Sci. 22 (5) (1991) 717–727.
[21] B. Coates, S.A. Argyropoulos, The effects of surface roughness and metal temperature on the heat-transfer coefficient at the metal mold interface, Metall. Mater. Trans. B: Process Metall. Mater. Process. Sci. 38 (2) (2007) 243–255.
[22] G. Dour, M. Dargusch, C. Davidson, Recommendations and guidelines for the performance of accurate heat transfer measurements in rapid forming processes, Int. J. Heat Mass Transfer 49 (11–12) (2006) 1773–1789.
[23] G. Dour, M. Dargusch, C. Davidson, A. Nef, Development of a non-intrusive heat transfer coefficient gauge and its application to high pressure die casting: Effect of the process parameters, J. Mater. Process. Technol. 169 (2) (2005) 223–233.
[24] C.W. Nelson, in: SDCE (Ed.), Transactions of 6th International Die Casting Congress & Exhibition, SDCE, Cleveland, OH, 1970, pp. 1–8.
[25] S. Hong, D.G. Backman, R. Mehrabian, Heat transfer coefficient in aluminum alloy die casting, Metall. Mater. Trans. B: Process Metall. Mater. Process. Sci. 10B (2) (1979) 299–301.
[26] J. Papai, C. Mobley, in: NADCA (Ed.), Transactions of the NADCA Congress, NADCA, Detroit, MI, 1991, pp. 377–384.
[27] J.V. Beck, Sequential estimation of thermal parameters, J. Heat Transfer 99 (2) (1977) 314–321.
[28] A. Hamasaiid, G. Dour, M. Dargusch, T. Loulou, C. Davidson, G. Savage, in: Charles-André Gandin, Michel Bellet (Eds.), Modeling of Casting, Welding and Advanced Solidification Processes – XI, Minerals, Metals and Materials Society, Opio, France, 2006, pp. 1205–1212.
[29] Z. Guo, S. Xiong, S.-H. Cho, J.-K. Choi, Development of an inverse heat transfer model and its application in the prediction of the interfacial heat flux, Jinshu Xuebao/Acta Metall. Sin. 43 (6) (2007) 607–611.
[30] L. Michalski, K. Echersdort, J. McGhee, Temperature Measurement, Wiley, New York, 1991. pp. 279–290.
[31] J.V. Beck, B. Blackwell, C.R.S. Clair, Inverse Heat Conduction: Ill-Posed Problems, Wiley, New York, 1985. pp. 125–134.
[32] J.V. Beck, B. Blackwell, A. Haji-Sheikh, Comparison of some inverse heat conduction methods using experimental data, Int. J. Heat Mass Transfer 39 (17) (1996) 3649–3657.
[33] R. Helenius, O. Lohne, L. Arnberg, H.I. Laukli, The heat transfer during filling of a high-pressure die-casting shot sleeve, Mater. Sci. Eng. A 413 (SI) (2005) 52–55.